NANOPOWDER ENGINEERING: FROM SYNTHESIS TO SINTERING. THE CASE OF ALUMINA-BASED MATERIALS

P. Palmero[1], V. Naglieri[1], M. Azar[2], V. Garnier[2],
M. Lombardi[1], L. Joly-Pottuz[2], J. Chevalier[2], L. Montanaro[1]

(1) *Department of Materials Science and Chemical Engineering, INSTM LINCE Lab., Politecnico di Torino, Corso Duca degli Abruzzi 24, 10129 Torino (Italy)*
(2) *Université de Lyon, INSA de Lyon, MATEIS UMR CNRS 5510, Bât. Blaise Pascal, 7 Av. Jean Capelle, 69621 Villeurbanne (France)*

E-mail: laura.montanaro@polito.it

Abstract

Nanostructuration of ceramic materials is a challenging way to improve their performances reliability and lifetime. However, a successful approach to the production of tailored ceramic nanostructures requires the development of innovative concepts at any step of the manufacturing chain, starting from the elaboration and processing of ceramic powders. This review is aimed to collect and discuss the major advancements achieved along this complex path, exploiting some history cases to illustrate the benefits resulting from a nanopowders engineering approach applied to the processing of ceramic powders.

Résumé

La nano-structuration des matériaux céramiques représente une voie prometteuse d'amélioration de leurs performances. Cependant, le succès dans les approches de fabrication de céramiques nano-structurées nécessite le développement de concepts innovants à tous les stades de la chaine d'élaboration, dès la synthèse ou la modification des poudres. Cette revue a pour but de collecter et de discuter des avancements réalisés dans ce domaine, en illustrant l'intérêt des approches d'ingénierie des nano-poudres céramiques.

Mots clés: Nanopowder, Sintering, Alumina, Zirconia, Nanocomposites.

1- INTRODUCTION: A BRIEF OVERVIEW OF CRITICAL ISSUES

The production of fully dense ceramic materials with nanosize features has received an increasing attention over the recent years in view of several industrial applications, because of the expected or even already achieved improvements in mechanical and/or functional performances.

However, a successful approach to nanostructuration requires the development of innovative concepts to be applied in each step of the ceramic manufacturing chain, starting from the tailoring of a suitable raw material, the ceramic powder.

Several synthesis routes have been therefore investigated and set up during the last decades (see, for instance, [1-5]) to supply suitable nanopowders having a variety of compositions and controlled characteristics. They refer to gas-phase as well as to wet chemical routes in the frame of the so-called bottom-up procedures, whereas solid state syntheses have been exploited for the so-called top-down approach, frequently assisted by high-energy milling processes [6-7]. In fact, depending on the synthesis routes, primary particles of the ceramic powders may be held together by weak ("soft") Van der Waals forces or by chemical ("hard") forces [8].

Also sintering of powders while retaining grain sizes in the nanometer range is a critical processing step, due to the inevitable coarsening tendency: grain growth out of the so-called nanometer regime ($\leq$ 100 nm) is really difficult to avoid. At the same time, consolidation of nanopowders presents additional challenges as compared to sintering of conventional powders, for instance due to possible retention of thermodynamically unstable phases (i.e., anatase instead of rutile for TiO_2, transition aluminas instead of alpha-phase for Al_2O_3, tetragonal instead of monoclinic ZrO_2) [9] as well as to agglomeration, able to limit a homogeneous particle packing during forming, thus negatively affecting the density and microstructure of the

green and consequently of the fired bodies [10-11].

The microstructure of green bodies obtained by forming agglomerated nanometric powders often present two types of pores: inter-agglomerate pores (of micronic size) and inter-crystallite pores (of nanometric size) within the agglomerate itself (Fig.1 [12]). During sintering, the elimination of the inter-agglomerate pores requires high temperatures, thus encouraging grain growth and ultimate loss of the nano-features [13-14].

Effective deagglomeration is therefore required. Ball milling has been extensively exploited, since it is a cheap, easy and effective process; however, contamination arising from the milling media has a great influence on the sintering behavior, frequently inhibiting the densification rate [15]. On the other hand, seeding nanocrystalline transition alumina powders with α-alumina milling ball abrasive seeds has been demonstrated to be a viable option for producing high-quality, fine-grained, alumina-based ceramics [16-19].

Forming of ultra-fine powders has been frequently oriented to methods exploiting colloidal processing, based on stable dispersion in liquid media [20], for instance promoted by suitable dispersant additions and/or proper pH conditions, leading to a substantial reduction or even elimination of the agglomerates.
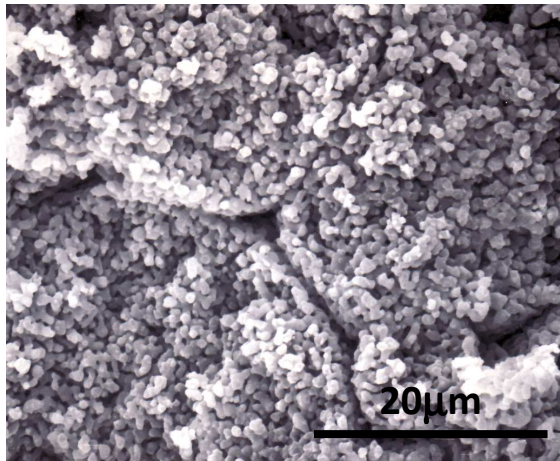
Fig.1: Quasi spherical agglomerates showing inter-agglomerate pores and inter-crystallite pores [12]

Many examples can be found in literature on the effectiveness of such colloidal approach in de-agglomeration and development of homogeneous, highly-performing microstructures: here, we just mention one paradigmatic experience performed in the elaboration of zirconia-toughened alumina ceramics [21]. Composites obtained by two different elaboration methods, precisely by a conventional powder mixing and by a colloidal route, were compared in terms of microstructural features (Fig.2 [21]) and mechanical response, demonstrating a paramount influence of the processing step and a significantly improved quality of the materials obtained via a colloidal approach.
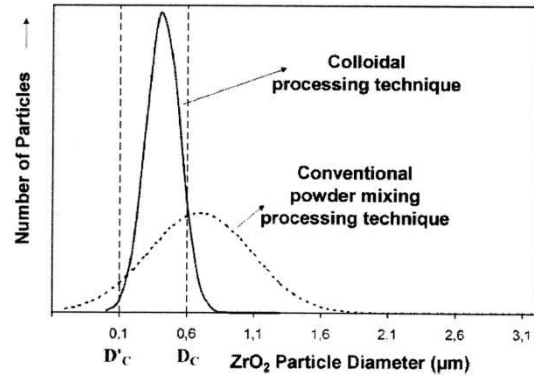
Fig.2: Comparison of the ZrO_2 particles size distribution in zirconia toughened alumina materials obtained by conventional powder mixing and colloidal processing route [21]

It must be also underlined that the positive effects on the final performances as well as the problems related to processing become more and more relevant if composite materials are considered (see, for instance, [22-32]).

Concerning the effect of the particle size distribution it has been demonstrated for submicronic alumina powder compacts [33] that, in the absence of agglomerates, a broader particle size distribution leads to two opposing phenomena during sintering, i.e., enhanced overall sintering characteristics and a higher degree of local differential densification. The former effect is the result of both the higher initial green density and smaller isolated pores in the final stage of sintering brought about the enhanced grain growth during the intermediate stage; the latter is promoted by a higher degree of variation in local particle packing and may negate the enhanced sintering effect at sufficiently broad particle size distribution. There therefore exists an optimum range of particle size distribution for best sinterability. However, since it may vary considerably even for a given powder, depending on the compaction technique and conditions used, narrow size distribution powders are preferable to monosized or broad size distribution powders for high sinterability and effective microstructural control of powder compacts, provided that agglomerates in the

starting powder are removed by appropriate means.

Dense components can be finally fabricated by using many processes, from pressure-less sintering or hot pressing or hot isostatic pressing to more innovative consolidation routes, like Spark Plasma Sintering (SPS, sometimes also referred as Pulse Electric Current Sintering (PECS)), each of them influenced by several operative parameters (see, for instance, [34-42]).

A two-step sintering concept, carried out by firstly heating to a higher temperature to achieve an intermediate density, followed by a cooling down and dwelling at a lower temperature for a long time until full densification is reached, has been successfully applied to nanostructured yttria materials [43]. However, such densification procedure seems not feasible for mass production processes due to heat transfer problems and temperature gradients at high heating rates in large-size industrial furnaces. However, a double-step pressure-less sintering approach [44-45], including a prolonged pre-sintering at low temperature before the final densification step at a higher temperature, was demonstrated effective in leading to a dense material, characterized by a very fine microstructure.

This review is devoted to deepen some of the aforementioned crucial aspects of processing and sintering of nanostructured alumina-based powders, being alumina ceramics widely used in a huge variety of engineering fields, because of their excellent chemical stability, electric properties, good mechanical performances, besides relatively low cost.

Two case-studies are here briefly discussed to highlight some of the progresses achieved and to illustrate potential outputs coming from the development of a systematic nanopowder engineering approach. It consists in the statement of a smart protocol for materials design and elaboration aimed to achieve the tailoring of the nanopowder features and of the nano/microstructural evolution through a strict control of the several processing steps involved on the path from the green body to the densified component.

2- TRANSITION ALUMINA NANOPOWDERS

The production of ultra-fine, dense α-Al_2O_3 ceramics from transition aluminas has been the subject of a considerable number of studies. Research was mostly aimed to understand and optimize dispersability, forming ability, and sinterability of nanosized transition alumina powders. The role of agglomeration on powder forming, and of the phase transition to α-Al_2O_3 as well of the dopants on the densification behavior has been extensively discussed: just few recent references among the many present in literature are here reported [13], [17], [33], [46-50].

From the above-mentioned studies, it is evident that metastable phase transformation into the thermodynamically stable α-Al_2O_3 during thermal sintering can play a crucial role, being accompanied with a rapid increase in the grain size [13].

The transformation proceeds by the formation of several increasingly ordered transition aluminas before final rearrangement into the stable phase α [51]. As an example, upon heating, γ-Al_2O_3 undergoes a series of polymorphic phase transformations from a highly disordered cubic close packed lattice to the more ordered cubic close packed θ-Al_2O_3. This sequence represents a so-called topotactic deformation. At higher temperatures, θ-Al_2O_3 undergoes a reconstructive transformation to form the thermodynamically stable hexagonal close packed α-phase. This transformation occurs by a nucleation and growth process [52]. The transformation into the stable α-Al_2O_3 is generally accompanied by the development of a vermicular microstructure enclosing a high proportion of intragranular pores (Fig.3).
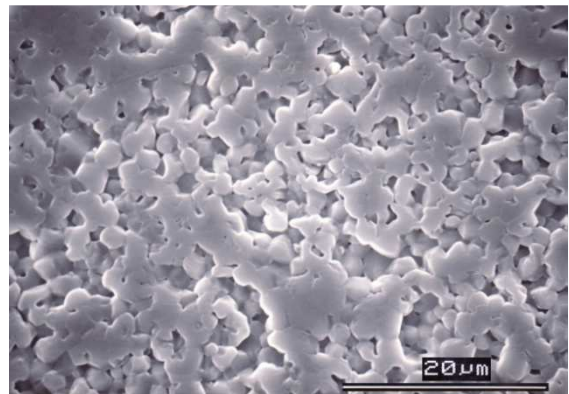
Fig.3: Micrograph of a vermicular microstructure induced by transition alumina transformation into α-phase during sintering

A quite simple model has been proposed to explain the appearance of such vermicular structure, in which coalescence of the α-alumina nuclei is firstly supposed, followed by growth due to migration when a critical size of the crystals is reached (Fig.4 [53]).

More recently [54], the possibility of eliminating the vermicular (also called finger)

growth of α-Al_2O_3 particles obtained by calcination of boehmite was also discussed.

Coalescence can imply a rearrangement mechanism of α-grains, which has been deeply discussed [48]. Vermicular structures are yielded by loose packing of transition alumina grains in which a re-arrangement do not take place (Fig. 5b); dense structures can be achieved from close packed systems (Fig.5a), but also in low-density green bodies, if a particle rearrangement can take place leading to an amplitude of the relative density variation for transformation ($\Delta\rho_R$) much higher than the simple crystallographic density change (of about 10%) (Fig. 5c).
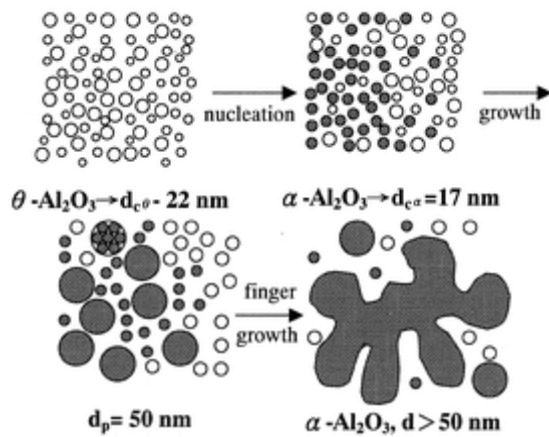
Fig.4:Scheme of a possible mechanism of θ- to α-phase transformation for an ultrafine alumina powder [53]
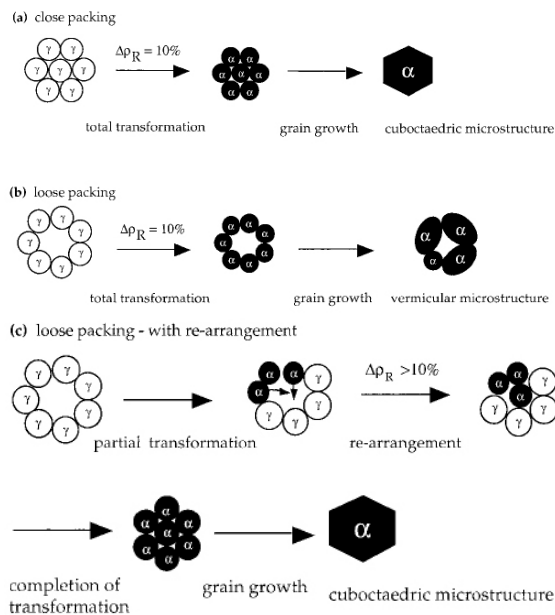
Fig.5: Scheme of the possible mechanisms leading to several transformation-induced α-alumina microstructures [48]

Mechanism (c) in Fig. 5 describes the transformation of transition alumina particles to α-phase, in a structure in which neighbouring grains are not close packed or not symmetrically arranged.

In such case, the crystallographic volume reduction, associated to the different theoretical densities of the two alumina phases, can induce non-symmetrical interparticle forces which can induce grains to slide and/or to rotate, leading to a rearrangement whose amplitude depends on the free space available and on the density of nucleation sites [48].

Recently [55] the effect of forming method (cold uniaxial pressing and slip casting) on particle packing and the consequent effects on densification, phase transformation and microstructural evolution were evaluated during sintering of a commercial transition alumina powder (Nanotek®, Nanophase Technologies corporation, Romeoville IL, US; particle size of 47 nm).
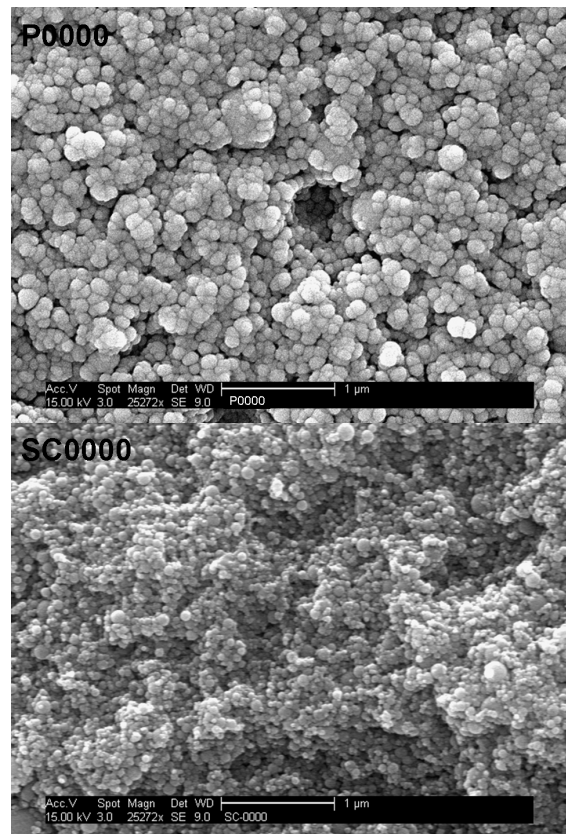
Fig.6: SEM (Scanning electron microscope) images of fracture surfaces of pressed (P0000) and slip-cast (SC0000) green compacts of NanoTek® powder

Green bodies with the same density (62%±1, of the true density – 3.49 g/cm^3 as

measured on the starting powder) were prepared, in order to investigate only particle packing homogeneity and its effect on phase transition and/or sintering (Fig.6).

Densification of transition alumina green bodies (Fig. 7) involves two major steps (denoted I and II hereafter). The first step of the densification (up to 1160° or 1200°C for SC and P specimens, respectively) coincides with the transformation of transition alumina to the thermodynamically stable α-alumina. The second step is associated to the sintering of α-alumina. Stage I for P specimens is divided into two 'sub-regions' (Ia and Ib), which may correspond to different stage in the transformation process of transition to stable alumina. Stage I is clearly shifted towards lower temperatures for SC specimens and is accompanied by a larger shrinkage. Stage II is more effective for SC materials, too. A clear maximum of densification rate is even observed for the SC samples (1400°C), which is usually hardly obtained on transition alumina without any seeding or doping aids.
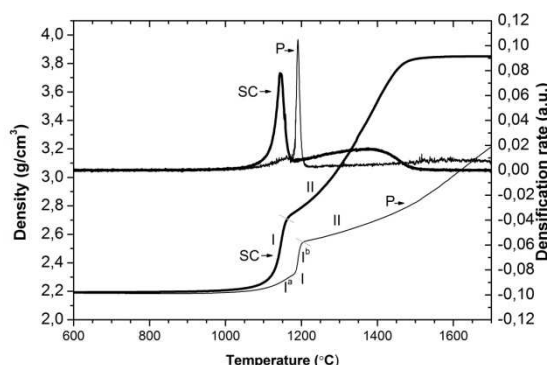
Fig.7: Density and densification rate versus temperature of pressed (P) and slip-cast (SC) compacts of NanoTek® powder from [55]

The higher homogeneity of particles distribution in the green compacts, achieved through dispersion in a liquid medium and then slip casting, promoted particle rearrangement during the phase transformation into the thermodynamically stable α-phase. As a consequence, a significant reduction of the phase transition temperature was observed in SC materials, as well as a drastic change in the microstructural evolution and in the quantity and the size of pores remaining after the transition, as shown in the SEM images of Fig. 8 and 9.

After sintering in air (heating rate of 5°C/min and cooling down to room temperature at 20°C/min) at 1400°C (Fig.8) the microstructure of SC is made of cuboctahedric grains, while that of P material is

still porous and vermicular. When the maximum densification temperature is raised up to 1700°C (Fig. 9), both materials present a cuboctahedral microstructure, but pores are still present in the pressed specimen.
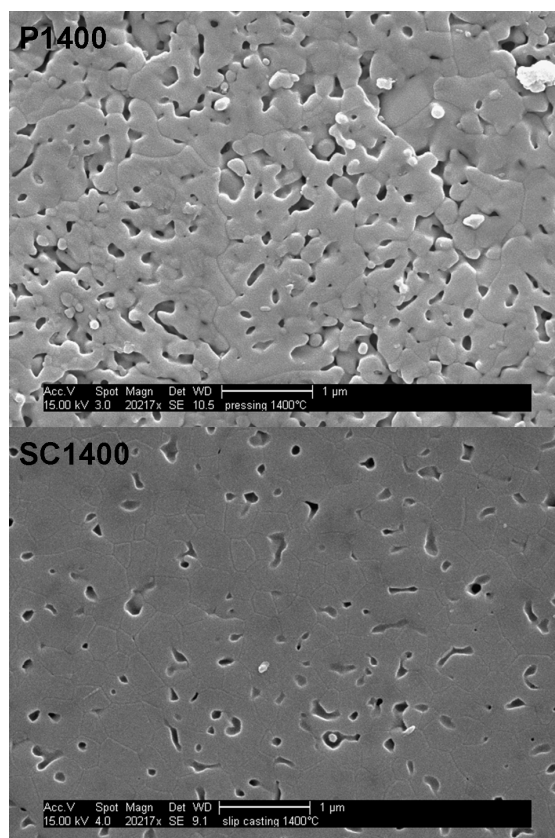
Fig.8: SEM micrographs of pressed (P) and slip-cast (SC) compacts of NanoTek® powder sintered at 1400°C

Therefore, the homogeneous distribution of porosity in the slip cast green compact limits the formation of α-Al_2O_3 with hard agglomeration or vermicular morphology and makes sintering to full density easier avoiding formation of large pores that are often entrapped within grains.

A major effect was also associated to the heating rate of the densification cycle [56], by carrying out a systematic investigation on uniaxially pressed compacts of the aforementioned transition alumina, ball-milled powders.

In fact, the phase and the microstructural evolution during sintering at different heating rates (10°C/min or 1°C/min) was followed by interrupting the thermal cycles at fixed temperatures, corresponding to the points evidenced in Fig. 10.

In this study it was noticed that a low-rate thermal cycle leads to a significant reduction of the α-Al_2O_3 crystallization temperature and

promotes a more effective particle rearrangement during phase transformation.
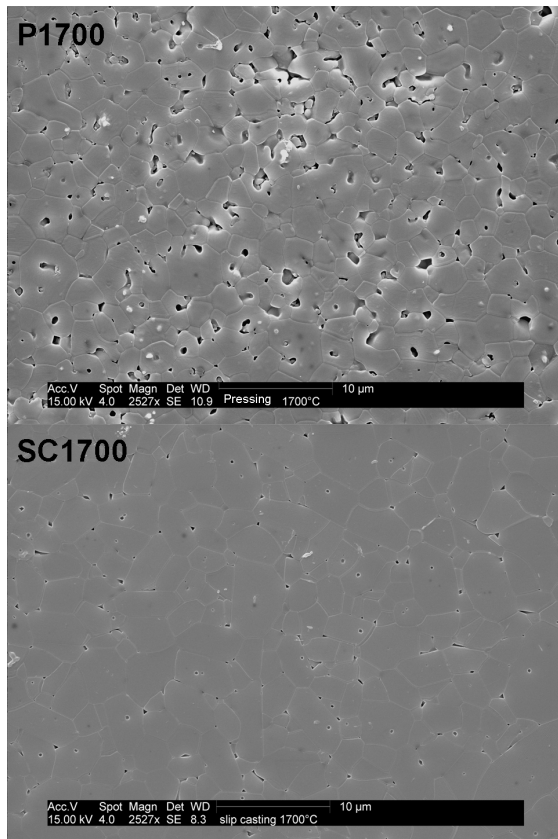
Fig.9: SEM micrographs of pressed (P) and slip-cast (SC) compacts of NanoTek® powder sintered at 1700°C
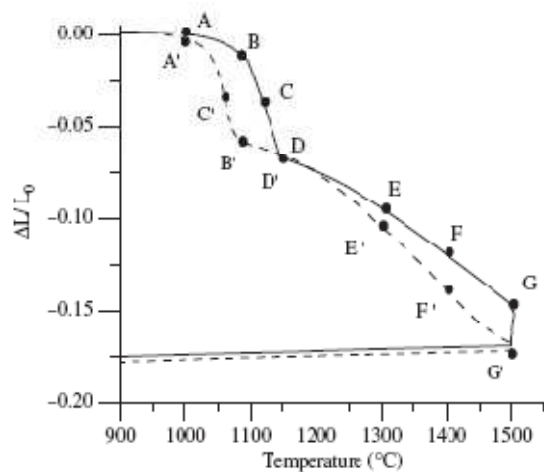
Fig.10: High-temperature segments of the densification curves up to 1500°C for 3 hours for NanoTek® compacts sintered at a heating rate of 10°C/min (solid line) or 1°C/min (dashed line) [56]

As a consequence, in the low-rate treated material, it was possible to avoid the development of a vermicular structure as usually expected during the densification of a transition alumina and to yield a more homogenously fired microstructure.

To summarize these results, in Fig. 11 it is possible to appreciate that the microstructures of the two materials started to significantly differ at 1135°C (points D and D' in Fig.10), even if they had reached almost the same shrinkage percentage.

The fast-rate-heated material presents a heterogeneous microstructure, consisting of agglomerates of ultrafine alumina particles of about 150–200nm, entrapping large porous areas. On the contrary, in the low-rate-heated one, a highly compact and homogenous structure, made of well-packed particles, was observed, and probably due to this better packing, more significant grain growth occurred.

(a)

(b)
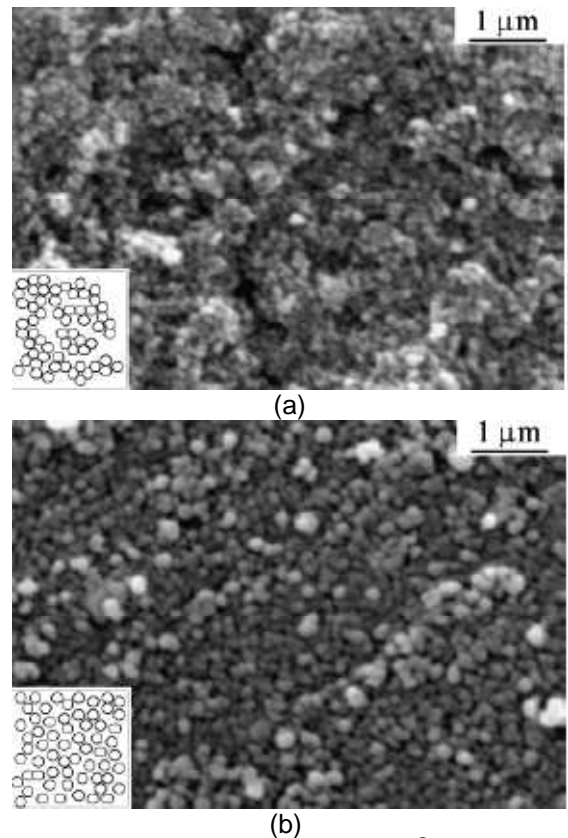
Fig.10: SEM images of NanoTek® compacts sintered at 1135°C at a heating rate of 10°C/min (a) or 1°C/min (b) [56]

As inserts to Fig.10, the schematic illustrations of the initial particle packing for green compacts obtained by pressing (a) and slip-casting (b) are reported, as proposed in another paper [55]. The microstructural evolution is quite similar, but here the difference is not imputable to the green-forming processes. In this case, therefore, an

easier and more effective particle rearrangement during transformation phenomena seems to be promoted by applying a lower heating rate, independently from the green packing efficiency, which is the same for both materials.

On the contrary, a faster heating rate did not allow such improvement of the packing density and homogenization of the microstructure during phase transformation, inducing the appearance of a vermicular structure and therefore leading to a lower sinterability.

3- ALUMINA-BASED NANOCOMPOSITES

3.1- Alumina-zirconia materials

Due to their excellent mechanical performances (hardness, strength, fracture toughness), alumina-zirconia composite are widely used (cutting tools, grinding media, wear parts, ...). They are raising interest in orthopaedics, since they exhibit a larger crack resistance than alumina and a lower sensitivity to aging than zirconia. Micro-nanocomposites in which tetragonal zirconia nanograins are embedded into a micron-sized alumina matrix are expected to exhibit improved slow crack growth resistance and stability [57].

Once again a crucial step is the preparation of alumina-zirconia composite powders. Several strategies have been exploited, from powder mixing to more or less complex chemical routes. A colloidal processing route in which alkoxides as precursors of the 2nd phase are added to a commercial alumina powder was demonstrated effective in producing dense and homogeneous alumina-based micro-nanocomposites [58].

More recently, an easier method based on inorganic precursors has been set-up and applied to several compositions [59-61]. Here the case of a 95 vol% alumina- 5 vol% zirconia composite, obtained through the surface modification of a commercial, ultra-fine alpha-alumina powder (TM-DAR TAIMICRON, Taimei Chemical Co., Japan; mean paricle size of 350 nm), is discussed [62].

After calcination at 500°C for 1 h, alumina grains are surrounded by an amorphous layer (Fig. 11a). Nano-sized zirconia crystallites are dispersed in the amorphous phase and only occasionally they are in contact with the alumina grains surface. These observations support a mechanism of homogeneous nucleation of zirconia crystallites into the amorphous phase, yielded by the precursor decomposition.

Increasing the calcinations temperature, the amorphous layer progressively disappears due to an improved crystallization. As a consequence, the zirconia nanocrystals are forced to approach the alumina grains surface, as witnessed by the HRTEM images collected on powders calcined at 600°C (Fig. 11b) and 1000°C (Fig. 11c).
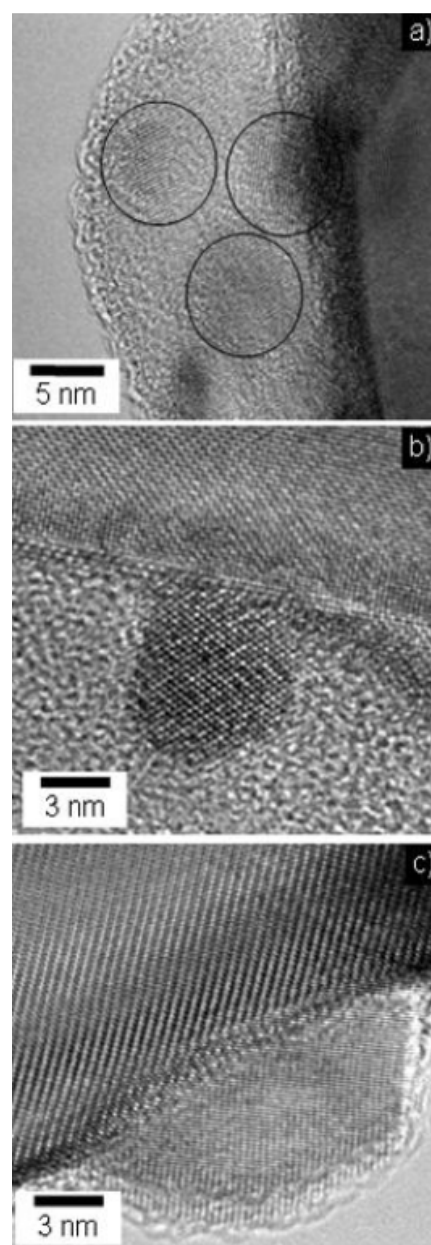
Fig.11: HRTEM images of the alumina-zirconia powder calcined at (a) 500°C, (b) 600°C, (c) 1000°C [62]

The evolution of the mean size of zirconia crystallites was followed as a function of temperature during isochronal treatments (Fig. 12). The growth rate is roughly independent of

the heating rate in the investigated range (1.5-30°C min^{-1}), but strongly affected by the temperature.

More details on the evolution of zirconia crystallite size were collected by performing a systematic investigation on powders heat treated in the temperature range 500°-1000°C (heating rate of 10°C/min; dwelling time of 1 h), by means of DF (Dark Field) and ADF (Annular Dark Field) TEM (Figure 13).
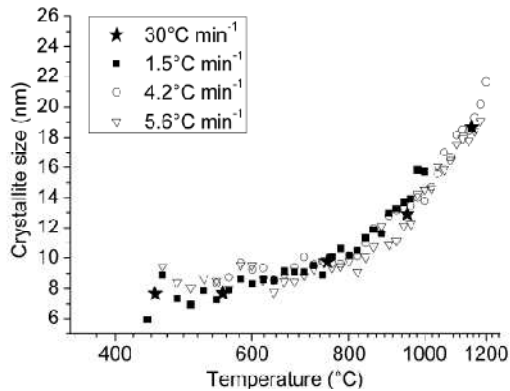
Fig.12: Zirconia crystallite size vs. time for the alumina-zirconia powder submitted to isochronal treatments in HT-XRD (several heating rates investigated) [62]

Moreover, a paramount influence of the dwelling time during calcination on the evolution of the final micro(nano)structure was shown. The soaking time seems to have a very poor influence on the crystallite growth in the low-temperature (500°-600°C) regimes, but prolonging the dwelling time an undesirable microstructural evolution was observed (Fig.14).

In fact, after calcination at 500°C for 1h, alumina grains are surrounded by an amorphous layer and small zirconia crystallite are present into this amorphous phase, as already stated by means of HRTEM. However, after a prolonged dwelling (10 h) at this temperature, microstructural regions richer in zirconia grains can be observed (see the arrow in Fig. 14b).

After treatment at 600°C, the thickness of the amorphous layer decreases and, if calcination is prolonged for 10 h, a similar trend than at 500°C is observed. Discrete amorphous phase pockets appear in which zirconia crystallites tend to agglomerate (see arrow in Fig.14d). Due to their low affinity to the alumina grains surface, the small zirconia crystallites are drained by the amorphous phase flow into discrete pockets in which they can start to aggregate. This is of primary importance since aggregation could lead to

coalescence and growth of the zirconia grains during sintering, hindering the microstructural control as well as the preservation of the nanostructure.
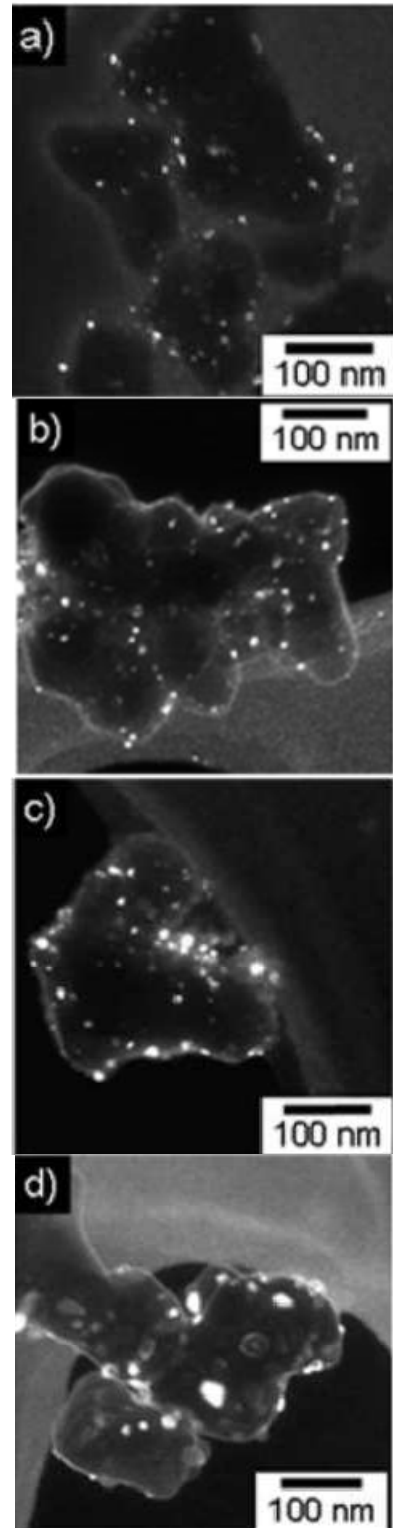
Fig.13:DF TEM images of the alumina-zirconia powder after calcination at different temperatures and times: a) 500°C-1 h, b) 600°C-1 h, c) 800°C-1 h, d) 1000°C-1h [62]
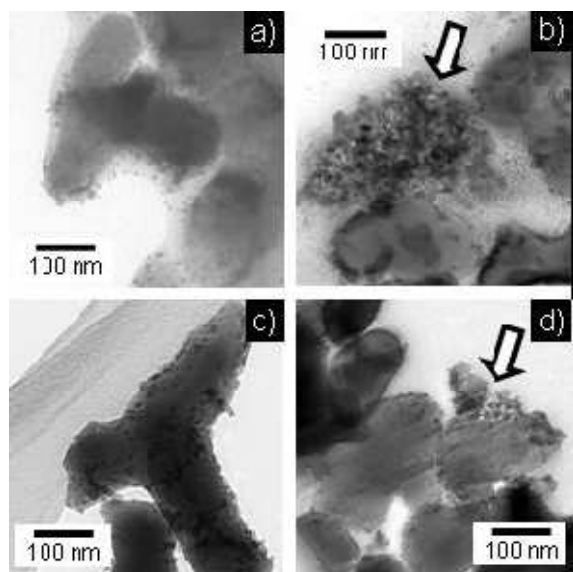
Fig.14: BF TEM images of the alumina-zirconia powder after calcination at different temperatures and times: a) 500°C-1 h, b) 500°C-10 h, c) 600°C-1 h, d) 600°C-10h [62]
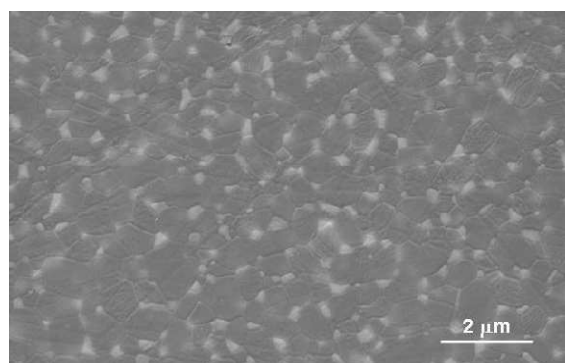
(a)
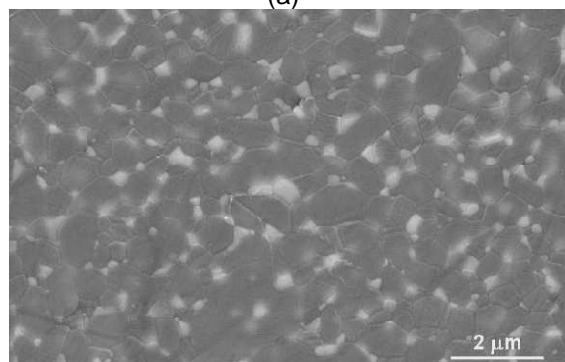
(b)

Fig.15: SEM images of alumina-zirconia sintered specimens obtained from powder pre-treated at 600°C for (a) 1 h, (b) 10 h [62]

This dramatic change at the nanopowder scale mirrored the evolution of the final microstructures in sintered materials densified at 1500°C for 3 h.

By comparing the SEM images of dense bodies obtained by composite powders treated at 600°C for 1h and 10 h, respectively (Fig. 15), it clearly appears that the finer and more homogeneous microstructure was developed starting from the powder calcined for the shorter time (1h).

Zirconia grain growth and heterogeneous distribution was observed in the sample obtained from the powder calcined for 10 h.

The above observations are confirmed by the data reported in Fig. 16, in which the zirconia grain size distributions of the afore-mentioned samples are compared. In the sintered material obtained by the powder calcined for a longer time, the zirconia grain size distribution is less homogeneous, resulting in a coarser microstructure.
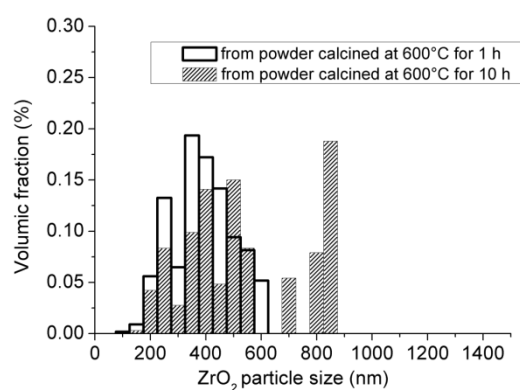
Fig.16: Zirconia grain size distribution in alumina-zirconia sintered specimens obtained from powder pre-treated at 600°C for 1 h or 10 h [62]

A possible scenario (Fig. 17) for the zirconia crystallization can be proposed starting from the collected results. After drying the modified powders are made of alumina grains coated with a layer of amorphous zirconia precursor.

Crystallization is then promoted by thermal treatments; by calcination at low temperature, a homogeneous nucleation of zirconia nano-crystals in the amorphous layer is already observed in the initial stage of the thermal treatment, while their growth rate is very slow, so that, at the intermediate stage, a slightly decrease of amorphous phase is observed, mainly imputable to continuous nucleation.

However, prolonging the treatment at low temperature, the amorphous phase, even if still present, is preferentially drained into discrete pockets among the alumina particles, to reduce the related contact surface.

Consequently, we hypothesize that the calcination time at low temperature could have

a dramatic effect on the final microstructure after sintering. In a first case, the powder calcined for short time contains uniformly distributed zirconia nuclei, so that, the resulting microstructure is homogeneous and a narrow size distribution of zirconia grains is obtained.
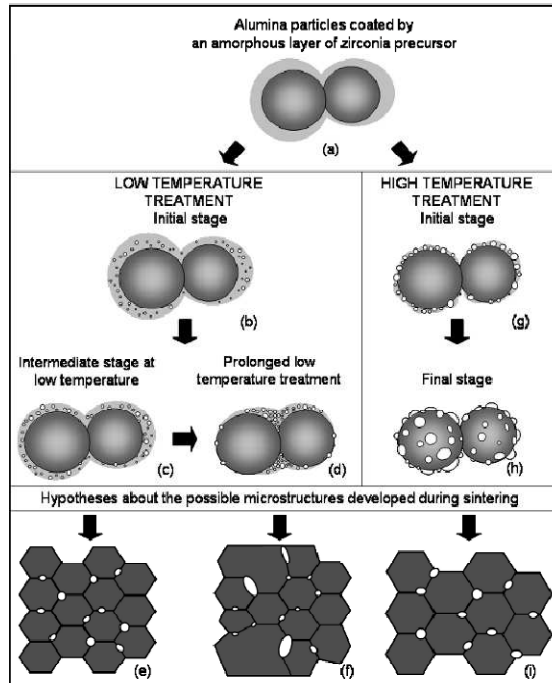
Fig.17: The Nanopowder Engineering Approach: settlement of the possible scenario of powder micro(nano)structural evolution and its impact on the quality of final material [62]

Otherwise, the powder calcined at low temperature for longer time contains zirconia nuclei preferentially located into pockets among the alumina particles where the amorphous phase is placed, and few isolated zirconia nano-grains.

This non-uniform morphology of the composite powder could reasonably give rise to an inhomogeneous microstructure in the sintered materials, where a bimodal distribution size of zirconia grains could be expected, being the larger grains originated by the coalescence of the close nuclei into pockets and the smaller ones by the isolated grains, and also abnormal grain growth could occur into the alumina matrix.

Instead, treating at high temperature, a faster crystallization takes place, the amorphous phase disappears at shorter times, comparing with the low temperature treatments, and crystal growth prevails over nucleation, so that larger zirconia crystals are yielded, homogeneously distributed onto the surface of the alumina particles.

In this case, the hypothesized microstructure of sintered bodies could be homogeneous, because the starting composite powder contains uniformly distributed zirconia on the alumina particles surface, but the mean grain size, both for the matrix and the second phase, is expected to be greater than in the case of materials obtained from the powder treated at low temperature for short time.

4- CONCLUSIONS

Sintering of nanostructured powders while retaining nanofeatures in the final, fully dense component is a complex exercise, more intricate when transition aluminas are involved.

It has been demonstrated that an effective dispersion of the powder and a proper choice of the forming process can lead to an improved homogeneity of the particles distribution in the green compact and hence to an enhancement of the particles rearrangement during the phase transformations into the thermodynamically stable α-phase.

This rearrangement produced a drastic change in the microstructural evolution and a significant reduction of the phase transition temperature as well as in the densification rate during sintering. Therefore, the homogeneous distribution of porosity in the slip cast green compact limits the formation of α-Al_2O_3 with hard agglomeration or vermicular morphology and makes sintering to full density easier, avoiding formation of large pores that are often entrapped within grains.

Also the heating rate was shown to play a major role during the two-step shrinkage path of the transition alumina, associated with a different phase evolution in the first step and a different microstructural development in the second one. A low-rate heating step promoted a more effective particle rearrangement during transformation to alpha- phase. As a consequence, a more homogeneous and well-packed microstructure developed during densification in the high-temperature regime.

Complexity increases when nanocomposite materials are considered. Discussing a case-study involving an alumina-zirconia micro-nanocomposite, it has been demonstrated that an effective tailoring of the final microstructural features is achievable by exploiting a rigorous protocol aimed at investigating step-by-step the ceramic processing, from the nanopowders synthesis to its sintering into a dense component.

Therefore, the development of a systematic nanopowder engineering approach

can successfully support ceramists in clearing the hurdle represented by nanostructuration.

REFERENCES

[1] D. Vollath, D.V. Szabo, J. Hausselt, Synthesis and properties of ceramic nanoparticles and nanocomposites, Journal of the European Ceramic Society, Vol. 17, N° 11, (1997), p. 1317-1324

[2] R.N. Das, P. Pramanik, Low temperature chemical synthesis of nanosized ceramic powders, British Ceramic Transaction, Vol. 99, N° 4, (2000), p. 153-158

[3] G. Skandan, A. Singhal, Tailoring nanostructured powders for functional and structural applications, Powder Metallurgy, Vol. 43, N° 4, (2000), p. 313-317

[4] J.A. Puszynski, Advances in the formation of metal and ceramic nanopowders, Powder Materials: Current Research and Industrial Practices, Vol.1, (2001), p. 89-105

[5] M. Winterer, H. Hahn, Nanoceramics by chemical vapour synthesis, Materials Research and Advanced Techniques, Vol. 94, N° 10, (2003), p. 1084-1090

[6] J. Li, F. Li, K. Hu, Y. Zhou, TiB_2/TiC nanocomposite powder fabricated via high energy ball milling, Journal of the European Ceramic Society, Vol. 21, N° 16, (2001), p. 2829-2833

[7] D.L. Zhang, Processing of advanced materials using high-energy mechanical milling, Progress in Materials Science, Vol. 49, (2004), p. 537-560

[8] R. Ge, Z. Liu, H. Chen, D. Zhang, T. Zhao, Wet-milling effect on the properties of ultrafine Yttria-stabilized Zirconia powders, Ceramis International, Vol. 22, (1996), p. 123-130

[9] J.R. Groza, Nanosintering, NanoStructured Materials, Vol. 12, (1999), p. 987-992

[10] F.F. Lange, Sinterability of agglomerated powders, Vol. 67, N°2, (1984), p. 83-89

[11] H. Ferkel, R.J. Hellmig, Effect of nanopowder deagglomeration on the densities of nanocrystalline ceramic green bodies and their sintering behaviour, NanoStructured Materials, Vol. 11, N°5, (1999) p.617-622

[12] L. Montanaro, A. Negro, Sintering behaviour of gel-derived powders, Journal of Materials Science, Vol. 26, (1991), 4511-4516

[13] P. Bowen, C. Carry, From powders to sintered pieces: forming, transformations and sintering of nanostructured ceramic oxides, Powder Technology, Vol. 128, (2002), p. 248-255

[14], A.V. Galakhov, Agglomerates in nanopowders and ceramic technology, Refractories and Industrial Ceramics, Vol. 50, N°5, (2009), 348-353

[15] F.-S. Shiau, T.-T. Fang, T.-H. Leu, Effects of milling and particle size distribution on the sintering behavior and the evolution of the microstructure in sintering powder compacts, Materials Chemistry and Physics, Vol. 57, (1998), 33-40

[16] M.L. Panchula, J.Y. Ying, Mechanical synthesis of nanocrystalline α-Al_2O_3 seeds for enhanced transformation kinetics, NanoStructured Materials, Vol. 9, (1997), p. 161-164

[17] C.S. Nordhal, G.L. Messing, Sintering of α-Al_2O_3-seeded nanocrystalline γ-Al_2O_3 powders, Journal of the European Ceramic Society, Vol. 22, (2002), p. 415-422

[18] Z.-P. Xie, J.-W. Lu, L.-C. Gao, W.-C. Li, L.-H. Xu, X.-D. Wang, Influence of different seeds on transformation of aluminum hydroxides and morphology of alumina grains by hot-pressing, Materials and Design, Vol. 24, (2003), p. 209-214

[19] Y. Yoshizawa, K. Hirao, S. Kanzaki, Fabrication of low cost fine-grained alumina powders by seeding for high performance sintered bodies, Journal of the European Ceramic Society, Vol. 24, (2004), p. 325-330

[20] N. Mandzy, E. Grulke, T. Druffel, Breakage of TiO_2 agglomerates in electristatically stabilised aqueous dispersions, Powder Technology, Vol. 160, (2005), p. 121-126

[21] A. H. De Aza, J. Chevalier, G. Fantozzi, Slow crack growth behavior of zirconia toughened alumina ceramics processed by different methods, Journal of the American Ceramic Society, Vol. 86, (2003), p. 115-120

[22] M. Sternitzke, Review: Structural ceramic nanocomposites, Journal of the European

Ceramic Society, Vol. 17, N° 9, (1997), p. 1061-1082

[23] S. Deville, J. Chevalier, G. Fantozzi, J.F. Bartolomé, J. Requena, J.S. Moya, R. Torrecillas, L.A. Diaz, Low-temperature ageing of zirconia-toughened alumina ceramics and its implication in biomedical implants, Journal of the European Ceramic Society, Vol. 23, N°15, (2003), p. 2975-2982

[24] Y. Luting, S. Wenjie, X. Tao, M. Hezhuo, Preparation of CIM feedstock of Al_2O_3-SiC nanocomposite, Key Engineering Materials, Vol.280-283, N°II, (2005), p. 1089-1092

[25] S. Mullens, J. Cooymans, C. Smolders, J. Luyten, Processing oxide-based nanocomposites, American Ceramic Society Bulletin, Vol. 84, N°1, (2005), on-line paper.
[26] J. Dusza, P. Sajgalik, Si_3N_4 and Al_2O_3 based ceramic nanocomposites, International Journal of Materials and Product Technology, Vol. 23, N°1-2, (2005), p. 91-119

[27] A. Mukhopadhyay, B. Basu, Consolidation-microstructure-property relationships in bulk nanoceramics and ceramic nanocomposites: A review, International Materials Review, Vol. 52, N° 5, (2007), p. 257-288

[28] R. Torrecillas, M. Schehl, L.A. Diaz, J.L. Menendez, J.S. Moya, Creep behaviour of alumina/YAG nanocomposites obtained by a colloidal processing route, Journal of the European Ceramic Society, Vol. 27, N° 1, (2007), p. 143-150

[29] R. Gadow, F. Kern, A. Killinger, Manufacturing technologies for nanocomposite ceramic structural materials and coatings, Materials Science and Engineering B: Solid-State Materials for Advanced Technology, Vol. 148, N°1-3, (2008), p. 58-64

[30] B. Zou, C.Z. Huang, H.L. Liu, M. Chen, Preparation and characterization of Si_3N_4/TiN nanocomposites ceramic tool materials, Journal of Materials Processing Technology, Vol. 209, N°9, (2009), p. 4595-4600

[31] H. Esfahani, A. Nemati, E. Salahi, The effects of composition and sintering conditions on zirconia toughened alumina (ZTA) nanocomposites, Advanced Materials Research, Vol. 93-94, (2010), p. 695-698

[32] M.H. Maneshian, M.K. Banerjee, Effect of sintering on structure and mechanical properties of alumina-15vol% zirconia nanocomposite compacts, Journal of Alloys and Compounds, Vol. 493, N° 1-2, (2010), p. 613-618

[33] J. Ma, L.C. Lim, Effect of particle size distribution on sintering of agglomerate-free submicron alumina powder compacts, Journal of the European Ceramic Society, Vol. 22, (2002), p. 2197-2208

[34] O. Vasylkiv, Y. Sakka, V. Skorokhod, Low-temperature sintering of zirconia and zirconia-alumina composite nano-powders, Key Engineering Materials, Vol. 206-213, N° I, (2001), p. 39-42

[35] A. Krell, H.-W. Ma, Sintering transparent and other sub-μm alumina: The right powder, CFI Ceramic Forum International, Vol. 80, N° 4, (2003), p. E-41-E-45+D32

[36] G.-D. Zhan, J.Kuntz, J. Wan, J. Garay, A.K. Mukjerjee, A novel processing route to develop a dense nanocrystalline alumina matrix (< 100 nm) nanocomposite material, Journal of the American Ceramic Society, Vol. 86, N°1, (2003), p. 200-202

[37] X. Zhou, D.M. Hulbert, J.D. Kuntz, R.K. Sadangi, V. Shukla, B.H. Kear, A.K. Mukherjee, Superplasticity of zirconia-alumina-spinel nanoceramic composite by spark plasma sintering of plasma sprayed powders, Materials Science and Engineering A, Vol. 394, N°1-2, (2005), p. 353-359

[38] J. Li, Y. Ye, Densification and grain growth of Al_2O_3 nanoceramics during pressureless sintering, Journal of the American Ceramic Society, Vol. 89, N°1, (2006), p. 139-143

[39] Y. Ye, J. Li, H. Zhou, J. Chen, Microstructure and mechanical properties of yttria-stabilized ZrO_2/Al_2O_3 nanocomposite ceramics, Ceramics International, Vol. 34, N° 8, (2008), p. 1797-1803

[40] A. Odaka, T. Yamaguchi, M. Hida, S. Taruta, K. Kitajima, Fabrication of submicron alumina ceramics by pulse electric current sintering using M^{2+} (M = Mg, Ca, Ni)-doped alumina nanopowders, Ceramics International, Vol. 35, N°5, (2009), p. 1845-1850

[41] S.A. Hassanzadeh -Tabrizi, E. Taheri-Nassaj, Compressibility and sinterability of Al_2O_3-YAG nanocomposite powder synthesized by an aqueous sol-gel method,

Journal of Alloys and Compounds, Vol. 506, N° 2, (2010), p.640-644

[42] M.Kim, R.M. Laine, Pressureless sintering t-zirconia-Al$_2$O$_3$ (54 mol%) core-shell nanopowders at 1120°C provides dense t-zirconia-toughened α-Al$_2$O$_3$ nanocomposites, Journal of the American Ceramic Society, Vol. 93, N°3, (2010), p. 709-715

[43] I.-W. Chen, X.-H. Wang, Sintering dense nanocrystalline ceramics without final-stage grain growth, Nature, Vol. 404, (200), p. 168-171

[44] F.J.T. Lin, L.C. De Jonghe, M.N. Rahaman, Microstructure refinement of sintered alumina by a two-step sintering technique, Journal of the American Ceramic Society, Vol. 80, N°9, (1997), p. 2269-2277

[45] R. Gadow, F. Kern, Pressureless sintering of injection molded zirconia toughened alumina nanocomposites, Journal of the Ceramic Society of Japan, Vol. 114, N° 11, (2006), p. 958-962

[46] E. Sato, C. Carry, Effect of powder granulometry and pre-treatment on sintering behavior of submicron-grained α-alumina, Journal of the European Ceramic Society, Vol. 15, (1995), p. 9-16

[47] S.J. Wu, L.C. De Jonghe, Sintering of Nanophase γ-Al$_2$O$_3$ powder. Journal of the American Ceramic Society, Vol. 79, N° 8, (1996), p. 2207-2211

[48] C. Legros, C. Carry, P. Bowen, H. Hofmann, Sintering of a transition alumina: effects of phase transformation, powder characteristics and thermal cycle, Journal of the European Ceramic Society, Vol. 19, (1999), p. 1967-1978

[49] F.S. Yen, J.L. Chang, P.C. Yu, Relationshipd between DTA and DIL characteristics of nanosized alumina powders during θ- to α-phase transformation, Journal of Crystal Growth, Vol. 246, (2002), p. 90-98

[50] P. Bowen, C. Carry, D. Luxembourg, H. Hofmann, Colloidal processing and sintering of nanosized transition aluminas, Powder Technology, Vol. 157, (2005), p. 100-107

[51] Y. Wang, C. Suryanarayana, L. An, Phase transformation in nanometer-sized γ-alumina by mechanical milling. Journal of the

American Ceramic Society, Vol. 88, (2005), p. 780–783.

[52] X. Yang, A. C. Pierre, D. R. Uhlmann, TEM study of boehmite gels and their transformation to α-alumina, Journal of non-Crystalline Solids, Vol. 100, (1988), p. 371–377.

[53] P.-L. Chang, F.-S. Yen, K.-C. Cheng, H.-L. Wen, Examinations on the critical and primary crystallite sizes during θ- to α-phase transformation of ultrafine alumina powders, NanoLetters, Vol. 1, N°5, (2001), p. 253-261

[54] P.-C. Yu, R.-J. Yang, Y.-T. Chang, F.-S. Yen, Fabrication of nano-scaled α-Al$_2$O$_3$ crystallite through heterogeneous precipitation of boehmite in a well-dispersed θ-Al$_2$O$_3$ suspension, Journal of the American Ceramic Society, Vol.9, N°8, (2007), p. 2340-2346

[55] M. Azar, P. Palmero, M. Lombardi, V. Garnier, L. Montanaro, G. Fantozzi, J. Chevalier, Effect of initial particle packing on the sintering of nanostructured transition alumina, Journal of the European Ceramic Society, Vol. 28, (2008), p. 1121-1128

[56] P. Palmero, M. Azar, M. Lombardi, J. Chevalier, G. Fantozzi, L. Montanaro, Effect of heating rate on phase and microstructural evolution during pressureless sintering of a nanostructured transition alumina, International Journal of applied ceramic technology, Vol, 6, N°3, (2009), p. 420-430

[57] A.H. De Aza, J. Chevalier, G. Fantozzi, M. Schehl, R. Torrecillas, Crack growth resistance of alumina, zirconia and zirconia toughened alumina ceramics for joint prostheses, Biomaterials, Vol. 23, (2002), p. 937-945

[58] M. Schehl, L.A. Diaz, R. Torrecillas, Alumina nanocomposites from powder-alkoxide mixtures, Acta Materialia, vol. 50, (2002), p. 1125-1139

[59] P. Palmero, V. Naglieri, J. Chevalier, G. Fantozzi, L. Montanaro, Alumina-based nanocomposites obtained by doping with inorganic salt solution: application to immiscible and reactive system. Journal of the European Ceramic Society, Vol. 29, (2009), p. 59-66.

[60] V. Naglieri, P. Palmero, L. Montanaro, Preparation and characterization of alumina-doped powders for the design of multi-phasic nano-microcomposites, Journal of Thermal

Analysis and Calorimetry, Vol. 97, (2009), p. 231-237

[61] P. Palmero, V. Naglieri, G. Spina, M. Lombardi, Microstructural design and elaboration of multiphase ultra-fine ceramics, Ceramics International (2010) in press (DOI: 10.1016/j.ceramint.2010.08.031)

[62] V. Naglieri, L. Joly-Pottuz, J. Chevalier, L. Montanaro, Follow-up of zirconia crystallization on a surface modified alumina powder, Journal of the European Ceramic Society, Vol. 30, (2010), p.3377-3387